Influence of Sputtered ZnO Seed Layer Thickness on the Nanostructural and Optical Properties of Li-Doped ZnO Nanorod Arrays

Xiao-Lan Tang[1], San-Lin Young[2,*], Chung-Yuan Kung[3], Ming-Cheng Kao[2],
Hone-Zern Chen[2], Chung-Jen Ou[2], Yong-Chang Jhang[3]

[1]*Department of Electronic Engineering, Suzhou Institute of Industrial Technology, Jiangsu Suzhou 215104, China*

[2]*Department of Electronic Engineering, Hsiuping University of Science and Technology, Taichung 41280, Taiwan*

[3]*Department of Electrical Engineering, National Chung Hsing University, Taichung 40227, Taiwan*

Abstract – The $Zn_{0.99}Li_{0.01}O$ nanorod arrays have been grown on the sputtered ZnO seed layer/ITO glass for nanostructural and optical properties investigation and on the sputtered ZnO seed layer/n-Si substrate for UV photodetection observation. Two different thickness of the ZnO seed layers were deposited by a sputtering system with the sputtering time of 1.5 and 3 minutes respectively. Then, vertical-aligned $Zn_{0.99}Li_{0.01}O$ nanorod arrays were grown by the low-temperature hydrothermal method. The x-ray diffraction patterns reveal that both nanorod arrays exhibit the same wurtzite structure with a preferential orientation along the c-axis. The FE-SEM images show that the length of the nanorod arrays increases obviously with increasing seed layer thickness. Besides, the photoluminescence spectra of both nanorod arrays show the same ultraviolet emission indicating the similar crystallite state with an optical bandgap of 3.28 eV and the slight decrease of visible emission indicating the insignificant decrease of defects. Finally, the I-V curves are measured in the dark and under UV illumination separately. The results show an increase of current variation ratio defined as $(I_{photo}-I_{dark})/I_{dark}$ with increasing ZnO seed layer thickness indicating an enhancement of ultraviolet photodetection characteristics which may be resulted from the increase of surface area due to the increase of nanorod length.

Keywords: zinc oxide; nanorod; seed layer; UV photodetection characteristics.

I. INTRODUCTION

Solid-state photodetectors based on compound semiconductors other than silicon opens new possibilities for commercial applications [1-2]. Compared with Si-based devices, ultraviolet (UV) photodetectors with wide bandgap semiconductors are especially attractive due to solar-blind ultraviolet detection property [3]. The compound semiconductor ZnO with a wide bandgap of 3.37 eV, high thermal stability, low-cost synthesis processes and compatibility with Si-based microelectronics makes itself become one of the most promising photonic materials for UV photodetection [4]. Recent researches further denoted that synthesis, characterization, and novel applications of the one-dimensional ZnO nanostructures have been intensive subjects due to their remarkable electrical, optical, and chemical properties [5]. Numerous researches have been reported on the ZnO-based UV detectors with one-dimensional nanostructures for the improvement of photonic characteristics [6]. Although ZnO-based one-dimensional nanostructures have been fabricated through various methods, the hydrothermal method offers more merits due to easier control of chemical composition and more simple method with a low-cost manufacturing process compared with other high vacuum fabrication processes [7]. For the application of ZnO-based semiconductors on electronic devices, the conventional method to produce *n*-type semiconductors is to dope elements with the group III or transitional metals in the ZnO-based compounds [8-9]. The *n*-type doped ZnO is known to be easily synthesized. However, the fabrication of the *p*-type ZnO-based optoelectronic devices has met the challenges of both low reproducibility and the lack of low-resistivity [10]. The *p*-type ZnO can be achieved by the doping of group I elements. In this study, the smaller element Li of the group I, compared with Zn, is designed to dope into the ZnO nanorods and two different thickness of the sputtered ZnO seed layers are designed to grow $Zn_{0.99}Li_{0.01}O$ nanorods for the investigation of the nanostructural and optical properties. Besides, the application of the $Zn_{0.99}Li_{0.01}O$ nanorod arrays on the seeded *n*-Si substrates for UV photodetection is also discussed.

II. EXPERIMENTAL

The $Zn_{0.99}Li_{0.01}O$ nanorod arrays were fabricated by the hydrothermal method on sputtered ZnO seeded ITO glasses and *n*-Si substrates with the sputtering time 1.5 and 3 minutes, respectively. The corning ITO glasses were ultrasonically cleaned in the acetone, ethanol, and deionized (DI) water each for 10 min successively. The *n*-Si substrates with 0.55 Ω·cm resistivity were also

ultrasonically cleaned in the acetone, ethanol, and deionized (DI) water each for 10 min successively and further wet etching step in HF (10%) solution was followed for 5 min to remove the native silicon oxide. Then, the *n*-Si substrates were rinsed in DI water and dried in flowing nitrogen gas. After the substrate cleaning processes, the sputtered ZnO seed layers with the sputtering time 1.5 and 3 minutes were separately deposited on the ITO glasses and *n*-Si substrates. The $Zn_{0.99}Li_{0.01}O$ nanorod arrays were grown on the ZnO-seeded ITO glass and *n*-Si substrates separately by the low-temperature hydrothermal method. The source solutions for $Zn_{0.99}Li_{0.01}O$ nanorod arrays growth were prepared with the precursors, including zinc acetate dehydrate $Zn(C_2H_3O_2)_2{\cdot}2H_2O$, lithium acetate dehydrate $LiCH_3COO{\cdot}2H_2O$ and hexamethylenetetramine $(CH_2)_6N_4$, in stoichiometric proportion dissolving in the DI water. Then, the seeded substrates were placed upside down into the solution contained in closed vials at 90°C for 1.5 h to grow the $Zn_{0.99}Li_{0.01}O$ nanorod arrays. Finally, the indium solder balls were pressed on the top of both the $Zn_{1-x}Li_xO$ nanorod arrays and the *n*-Si substrates to the measure the I-V curves.

The crystal structure of both $Zn_{0.99}Li_{0.01}O$ nanorod arrays was determined by the x-ray diffraction (XRD) patterns using a Rigaku D/max 2200 x-ray diffractometer with Cu-Kα radiation. The XRD data were recorded in the 2θ range from 20° to 60° with a step width of 0.01° and a scan speed of 0.5°/min. The surface morphologies and cross-section images of the nanorods were observed by a field emission scanning electron microscope (FE-SEM, JEOL JSM-6700F) at 3.0 kV. Then, photoluminescence (PL) spectrometer was used to measure the optical emissions of both $Zn_{0.99}Li_{0.01}O$ nanorod arrays from 330 to 645 nm by a 325 nm He-Cd laser. Finally, the current-voltage (I-V) curves of both $Zn_{0.99}Li_{0.01}O$ nanorod arrays with the bias voltage from -5 V to 5 V were performed in the dark and under UV illumination using the two-point probe I-V curve method with a Keithley 2400 source meter.

III. RESULTS AND DISCUSSION

Fig. 1 shows the FE-SEM top view and cross section images of the $Zn_{0.99}Li_{0.01}O$ nanorod arrays grown on the sputtered ZnO seed layer/ITO glass with the sputtering time 1.5 and 3 minutes of the ZnO seed layers, respectively. The length of the nanorods increases from 1303.1 to 1656.6 nm with increasing the sputtered ZnO seed layer thickness. The result indicates the increase of seed layer will enhance the growth rate of $Zn_{0.99}Li_{0.01}O$ nanorod arrays.

Fig. 2 shows the XRD patterns of the $Zn_{0.99}Li_{0.01}O$ nanorod arrays. As the XRD patterns shown, the $Zn_{0.99}Li_{0.01}O$ nanorod arrays are found to have the same wurtzite hexagonal structure with space group P63/mc.

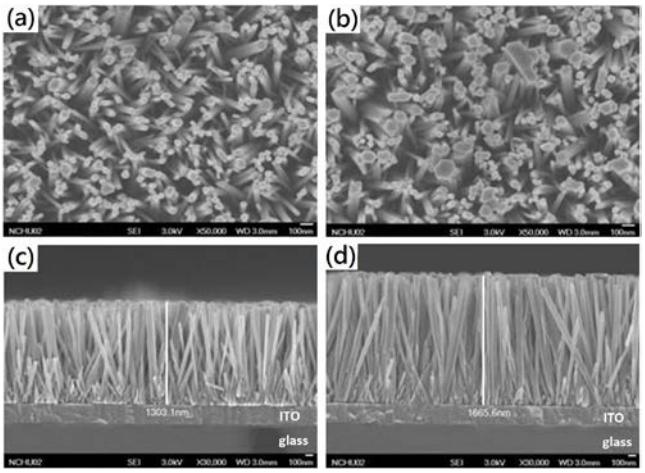

Fig. 1 FE-SEM top view images of the $Zn_{0.99}Li_{0.01}O$ nanorod arrays grown on the sputtered ZnO seed layer/ITO glass with sputtering time (a) 1.5 and (b) 3 minutes of the ZnO seed layers. FE-SEM cross-section images with sputtering time (c) 1.5 and (d) 3 minutes of the ZnO seed layers.

Except for the ITO diffraction peaks, the higher peaks intensity of the ZnO nanorod arrays with a longer sputtering time of the ZnO seed layer indicates the enhancement of crystal growth rate and the corresponding increase of nanorods length. The result is consistent with the results observed from the FE-SEM images.

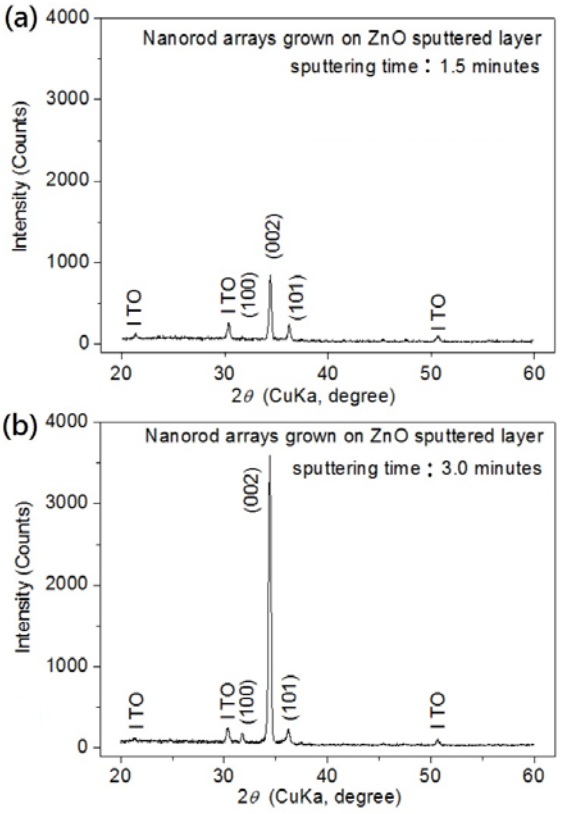

Fig. 2 The $Zn_{0.99}Li_{0.01}O$ nanorod arrays grown on the sputtered ZnO seed layer/ITO glass with sputtering time (a) 1.5 and (b) 3 minutes of the ZnO seed layers.

Fig. 3(a) shows the PL spectra of both $Zn_{0.99}Li_{0.01}O$ nanorod arrays grown on the sputtered ZnO seed layer/ITO glass with sputtering time (a) 1.5 and (b) 3 minutes of the ZnO seed layers. As shown in the Fig. 3(a), the, there is a strong emission peak at 377.6 nm in UV band and a weak broad-band emission peak at 525 nm (green) in the visible band. The UV emission peak is originated from excitonic recombination corresponding to the near-band-edge emission and the green emission is attributed to the recombination of electrons trapped in single ionized oxygen vacancies with holes [11]. In particular, the PL spectra of both $Zn_{0.99}Li_{0.01}O$ nanorod arrays grown on the sputtered ZnO seed layer/ITO glass with the sputtering time 1.5 and 3 minutes of the ZnO seed layers are almost overlap indicating the same crystallite state with an optical bandgap of 3.28 eV calculated by the formula, E_g=1240/λ. However, a slight decrease of visible emission at about 525 nm indicating an insignificant decrease of oxygen defects.

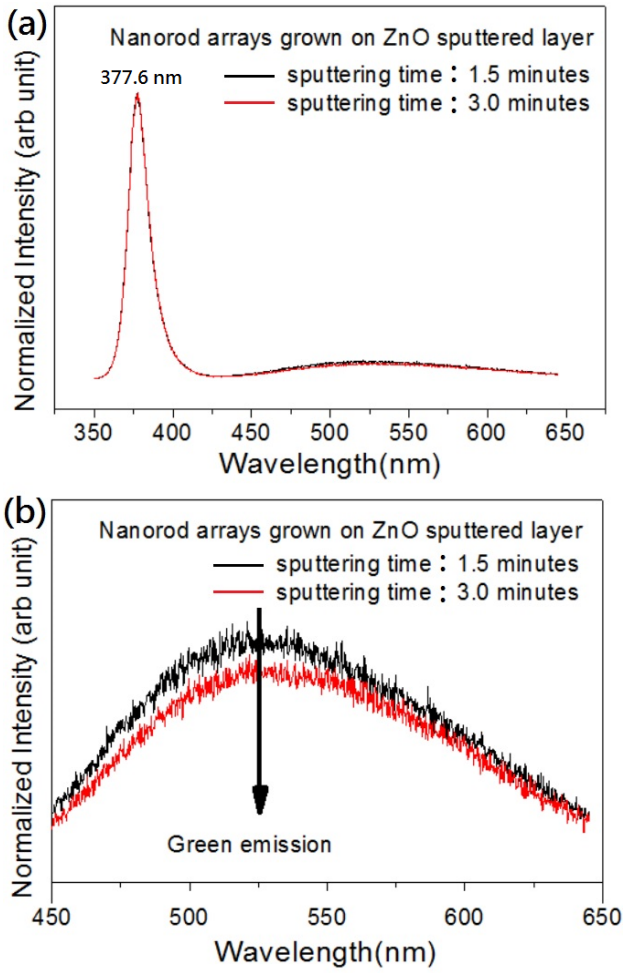

Fig. 3 (a) Photoluminescence spectra of the $Zn_{0.99}Li_{0.01}$ nanorod arrays grown on the ZnO sputtered seed layer with the sputtering time 1.5 and 3 minutes. (b) Enlarged photoluminescence spectra within 450 and 645 nm for visible emission comparison.

Figure 4 shows the I-V curves of the $Zn_{0.99}Li_{0.01}$ nanorod arrays grown on the sputtered ZnO seed layer/*n*-Si substrates with the sputtering time 1.5 and 3 minutes of the ZnO seed layers. The I-V curves were measured in the dark (dark-current, noted as I_{dark}) and under UV illumination (photo-current, noted as I_{photo}), respectively, for the exploration of the UV photodetection application. As listed in Table 1, the I_{dark} obviously decreases from 25.39 to 14.11 mA with the increase of ZnO seed layer sputtering time from 1.5 to 3 minutes, due to the increase of resistance resulted from the increase of nanorods length. However, the I_{photo} increases obviously from 96.92 to 161.53 mA with the increase of ZnO seed layer sputtering time from 1.5 to 3 minutes, due to the obvious increase of nanorods length resulting in a largely increase of UV light-absorption surface area and the corresponding increase of UV light induced electron-hole pairs.

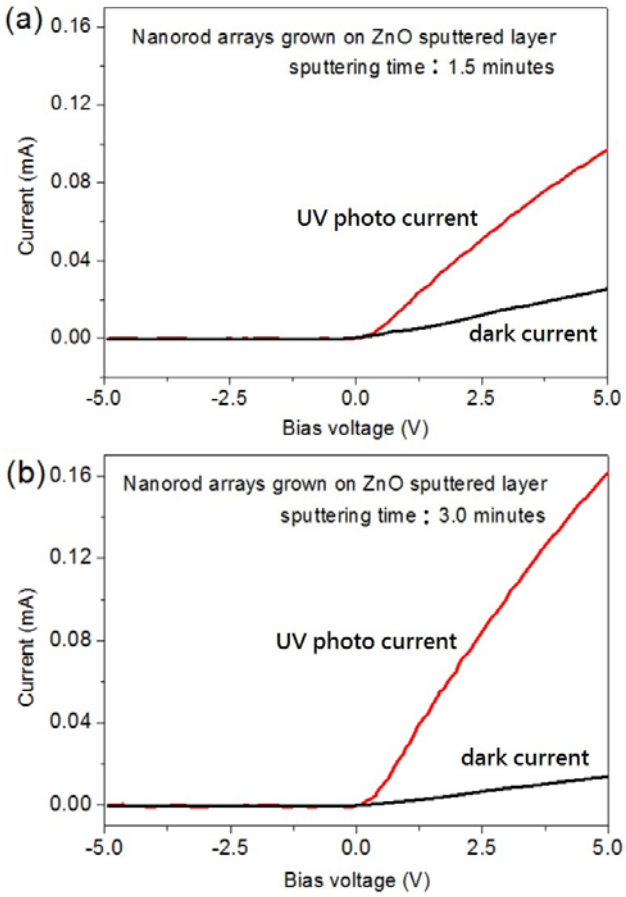

Fig. 4 I-V curves in the dark and under UV illumination of the $Zn_{0.99}Li_{0.01}O$ nanorod arrays/ZnO seeded *n*-Si photodetection structure with sputtering time (a) 1.5 and (b) 3 minutes of the ZnO seed layers.

Meanwhile, an obvious increase of current under UV illumination than that of in the dark is observed. The I_{dark} and I_{photo} current values measured at 5V along with UV photo-induced current variation ratio (R) of the $Zn_{0.99}Li_{0.01}O$ nanorod arrays in Table 1. The UV photo-induced current variation ratio is defined as $(I_{dark}-I_{photo})/I_{dark}$ at 5V bias voltage to evaluate the UV photodetection characteristic. Due to the obviously decrease of I_{dark} and increase of I_{photo} with the sputtering time of the ZnO seed layer, the R increases apparently

from 281.73% to 1044.79%. As a result, we obtain an obviously increased UV photo-induced current variation ratio (R) with increasing seed layer sputtering time which illustrates the possibility for photodetection application.

TABLE 1. Dark and photo current values measured at 5V along with current variation ratio of the $Zn_{0.99}Li_{0.01}O$ nanorod arrays.

Sputtering time (minute)	I_{dark} (μA)	I_{photo} (μA)	R (%)
1.5	25.39	96.92	281.73
3.0	14.11	161.53	1044.79

IV. CONCLUSION

The influence of sputtered ZnO seed layer thickness on the nanostructural, optical and electrical properties of the $Zn_{0.99}Li_{0.01}O$ nanorod arrays and corresponding application on the UV photodetection are investigated in this study. The length of the nanorods increases with increasing the thickness of the sputtered ZnO seed layer. Both XRD patterns of the $Zn_{0.99}Li_{0.01}O$ nanorod arrays reveal the same hexagonal wurtzite structure. PL spectra show the similar crystallite state with the same optical bandgap of 3.28 eV. From the I-V measured results, the UV photo-induced current variation ratio increase apparently from 281.73% to 1044.79% with the sputtering time 1.5 and 3 minutes of the sputtered ZnO seed layer, respectively, which shows the possibility for UV photodetection application.

ACKNOWLEDGMENT

This work was sponsored by the Ministry of Science and Technology of the Republic of China under the grant No. MOST 105-2221-E-005-040.

REFERENCES

[1] S.C. Dhanabalan, J.S. Ponraj, H. Zhang and Q. Bao, “Present perspectives of broadband photodetectors based on nanobelts, nanoribbons, nanosheets and the emerging 2D materials”, Nanoscale Vol. 8, pp. 6410-6434, 2016.

[2] F.H.L. Koppens, T. Mueller, Ph. Avouris, A.C. Ferrari, M.S. Vitiello and M. Polini, “Photodetectors based on graphene, other two-dimensional materials and hybrid systems”, Nat. Nanotechnol. Vol. 9, pp. 780-793, 2014.

[3] H. Chen, K. Liu, L. Hu, A.A. Al-Ghamdi and X. Fang, “New concept ultraviolet photodetectors”, Mater. Today Vol. 18, pp. 493-502, 2015.

[4] W. Tian, H. Lu, L. Li, “Photodetectors: materials, devices and applications”, Nano Res. Vol. 8, pp. 382-405, 2015.

[5] S.M. Ahmad and J. Zhu, “ZnO based advanced functional nanostructures: synthesis, properties and applications“, J. Mater. Chem. Vol. 21, pp. 599-614, 2011.

[6] C.-H. Chen and C.-T. Lee, “High detectivity mechanism of ZnO-based nanorod ultraviolet photodetectors”, IEEE Photon. Tech. Lett. Vol. 25, pp. 348-351, 2013.

[7] S.-J. Young, C.-C. Yang and L.-T. Lai, “Review-growth of Al-, Ga-, and In-doped ZnO nanostructures via a low-temperature process and their application to field emission devices and ultraviolet photosensors”, J. Electrochem. Soc. Vol. 164, pp. B3013-B3028, 2017.

[8] S.H. Jeong, B.N. Park, S.-B. Lee and J.-H. Boo, “Study on the doping effect of Li-doped ZnO film”, Thin Solid Films Vol. 516, pp. 5586-5589, 2008.

[9] J.G. Reynolds and C.L. Reynolds, “Progress in ZnO acceptor doping: What is the best strategy”, Adv. Cond. Matter. Phys. Vol. 2014, pp. 457058-1-15, 2014.

[10] O. Maksimov, “Recent advances and novel approaches of p-type doping of ZnO”, Rev. Adv. Mater. Sci. Vol. 24, pp. 26-34, 2010.

[11] C.C. Lin, S.L. Young, C.Y. Kung, H.Z. Chen, M.C. Kao, L. Horng, and Y.T. Shih, “Structural dependence of photoluminescence and room-temperature ferromagnetism in lightly Cu-doped ZnO nanorods”, IEEE Trans. Magn. Vol. 47, 3366-3368, 2011.